Molecular Biology Reports (2026) 53:1948
https://doi.org/10.1007/s11033-026-13097-8

BRIEF REPORT

Transcriptomic changes associated with the antiproliferative effects of indole-3-acetic acid in SH-SY5Y neuroblastoma cells: an exploratory study

Stefano Varriale[1] · Maria Laura Amenta[1] · Rosa Merlo[1] · Rosanna Mattosovich[1] · Marta Mallardo[2,3] · Ersilia Nigro[2,4] · Aurora Daniele[2,5] · Anna Valenti[1] · Carmelina Bianco[1]

Received: 29 July 2026 / Accepted: 27 October 2026
© The Author(s), under exclusive licence to Springer Nature B.V. 2026

Abstract

Background Neuroblastoma is a highly heterogeneous paediatric malignancy characterized by dysregulated oncogenic pathways that promote tumor progression and therapeutic resistance. We previously demonstrated that indole-3-acetic acid (IAA), a naturally occurring indole derivative, exerts antiproliferative effects in SH-SY5Y and SK-N-BE(2) neuroblastoma cells by reducing cell viability, downregulating ALK expression, inducing G1 cell-cycle arrest, promoting autophagy, and suppressing clonogenicity and migration.

Methods and Results To explore molecular correlates of these effects, we analysed the transcriptomic response of SH-SY5Y neuroblastoma cells to IAA treatment by RNA sequencing (RNA-seq), followed by differential expression analysis and Gene Ontology (GO)-based Gene Set Enrichment Analysis (GSEA). RNA-seq identified concentration-dependent transcriptional responses to IAA treatment, with the most pronounced changes observed at 1 mM concentration. GSEA identified neuronal migration as a significantly enriched biological process, suggesting modulation of developmental programs associated with the neural origin of neuroblastoma cells. Among the differentially expressed genes, *ERBB4* and *GPM6A* showed reduced expression and *MAMDC2* displayed increased expression following IAA treatment, changes that were confirmed by qRT-PCR in independent biological samples. *ADGRG1*, *FER1L4* and *DCDC2* were not confirmed by qRT-PCR and are reported as RNA-seq observations only. *ALK* transcript levels remained unaffected, raising the hypothesis that reduced ALK protein levels may involve post-transcriptional regulation, although this was not directly tested in the present study. *ERBB4*, *MAMDC2* and *GPM6A* are involved in cancer-related signalling and cellular behaviour, and their modulation by IAA has not been previously described.

Conclusion These findings show that IAA induces extensive transcriptional changes in SH-SY5Y cells and identify candidate molecular correlates of its antiproliferative activity. This exploratory, hypothesis-generating study is limited to transcript-level data from a single cell line. It provides a dataset and candidate genes for future validation and mechanistic studies in neuroblastoma models with different molecular backgrounds.

Keywords ″Indole-3-acetic acid · Neuroblastoma · SH-SY5Y · RNA-seq · Neuronal migration · Transcriptional reprogramming

✉ Anna Valenti
anna.valenti@cnr.it

✉ Carmelina Bianco
carmelina.bianco@cnr.it

[1] Institute of Biosciences and Bioresources (IBBR), National Research Council of Italy (CNR), Via Pietro Castellino 111, Napoli 80131, Italy

[2] CEINGE-Biotecnologie Avanzate Scarl ″Franco Salvatore″, Via G. Salvatore 486, Napoli 80145, Italy

[3] Dipartimento di Scienze dell'educazione e dello Sport, Centro Direzionale Isola F2, Università Telematica Pegaso, Naples 80143, Italia

[4] Dipartimento di Scienze e Tecnologie Ambientali, Università della Campania ″Luigi Vanvitelli″, Via Vivaldi 43, Biologiche, Farmaceutiche, Caserta 81100, Italy

[5] Dipartimento di Medicina Molecolare e Biotecnologie Mediche, Università di Napoli ″Federico II″, Via Pansini 5, Napoli 80138, Italy

Introduction

Neuroblastoma (NB) is the most common extracranial solid tumor in paediatric patients. It arises in early childhood from neural crest-derived progenitor cells of the sympathetic nervous system, a developmental context characterized by high proliferative and migratory activity that increases susceptibility to oncogenic transformation [1]. NB is a biologically and genetically heterogeneous disease whose clinical and biological heterogeneity remains only partially explained despite substantial advances in understanding its genomic and transcriptional landscape; its clinical variability is driven by diverse genomic alterations and transcriptional programs affecting tumor progression and therapeutic response [2]. In addition, neuroblastoma cells display marked phenotypic plasticity mediated by transcriptional and epigenetic reprogramming, which contributes to disease progression and treatment resistance; key oncogenic drivers, including *MYCN*, *LIN28B*, *PHOX2B*, and *ALK*, further disrupt normal developmental pathways controlling proliferation and differentiation [3].

In this context, we previously demonstrated that treatment with indole-3-acetic acid (IAA) exerted a consistent antitumor effect in neuroblastoma cells [4]. Specifically, IAA significantly reduced cell viability and clonogenic potential, induced a marked G1-phase cell-cycle arrest, enhanced autophagic activity, and impaired cell migratory capacity. These effects were accompanied by a downregulation of ALK expression, suggesting a potential link between IAA exposure and modulation of key oncogenic signalling in neuroblastoma.

To explore molecular correlates of the antiproliferative activity of IAA, we analysed the transcriptomic profile of treated SH-SY5Y neuroblastoma cells by RNA sequencing. Given the neural crest origin of neuroblastoma and the persistence of developmental programs regulating migration, pathway analysis may identify effects of IAA on processes associated with tumor progression and cellular plasticity.

Among the differentially expressed genes, *ERBB4*, *ADGRG1*, *FER1L4*, and *MAMDC2* were selected based on their reported roles in cancer-related signalling and processes relevant to proliferation, adhesion, and migration [5–8]; gene associated with neuronal migration (*DCC*, *GPM6A*, *DCDC2*) were also examined. We therefore investigated IAA-induced transcriptional changes using RNA-seq and GO-based GSEA and examined whether their expression changes are associated with the antiproliferative and antimigratory phenotype previously observed. This exploratory study is limited to transcript-level data in a single cell line.

Materials and methods

Cell culture and treatment

The human neuroblastoma SH-SY5Y cell line was kindly provided by the Bank of Human and Animal Continuous Cell Lines-CEINGE Biotecnologie Avanzate "Franco Salvatore", Napoli, Italy. The SH-SY5Y cells were cultured in DMEM purchased from Thermo Fischer Scientific, supplemented with 10% fetal bovine serum (FBS) (Lonza, Basel, Switzerland), 1% l-glutamine (Sigma-Aldrich, MO, USA), and 1% penicillin/streptomycin (Thermo Fischer Scientific, Massachusetts, USA). Cells were grown in a humidified 5% CO_2 incubator at 37 °C and used within passages 26–32. Cells incubated in medium alone served as the negative control. All experiments were conducted in 5% FBS medium following a 12-hour starvation period. For the IAA treatment, IAA was dissolved in DMSO and cells were treated at final concentrations of 0.1 mM and 1 mM for 48 h. These concentrations were selected based on our previous dose-response characterization of IAA effects in SH-SY5Y cells, in which a broader concentration range (0.01–1 mM) was tested and antiproliferative, cell-cycle, autophagic, and migratory effects were shown to increase in an IAA concentration-dependent manner across this range [4]. Millimolar concentrations of IAA are consistent with those employed in previous studies characterizing its biological and structural/functional properties in vitro [9].

Untreated control cells were incubated with medium containing the same concentration of DMSO for the same duration. At the end of the treatment period, 1×10^6 cells were harvested for each sample and stored in RNA stabilization buffer prior to RNA extraction.

Total RNA samples were extracted and processed for transcriptomic analysis by Eurofins Genomics (Ebersberg, Germany).

RNA sequencing and bioinformatic analysis

Raw RNA sequencing reads were processed using a standardized bioinformatics pipeline. Ribosomal RNA (rRNA) reads were removed using RiboDetector [10], and sequence quality was assessed using fastp [11] by trimming adapter sequences, removing low-quality bases (Phred score < 20), and discarding reads shorter than 30 bp. Only high-quality reads passing quality control were retained for downstream analyses. High-quality reads were aligned to the Homo sapiens reference genome (GRCh38/hg38, UCSC) using STAR (v2.7.10b) [12]. Gene-level expression was quantified using RSEM (v1.3.3), generating expected read counts for downstream analyses.

Differential gene expression analysis was performed using DESeq2 [13]. Genes with fewer than 10 reads on average across experimental groups were removed before analysis. DESeq2 was used for read count normalization and identification of differentially expressed genes between conditions. Statistical significance was assessed using the Benjamini–Hochberg false discovery rate (FDR) correction. Genes with an adjusted p-value ≤ 0.1 and an absolute log2 fold change > 1 were considered significantly differentially expressed.

Principal component analysis (PCA) and volcano plots were generated in R (v4.6.0). PCA was performed on variance-stabilized expression data generated using the DESeq2 variance stabilizing transformation (VST) to evaluate global transcriptomic variation among experimental groups, whereas volcano plots were generated using the complete differential expression dataset by plotting $\log_2$ fold change values against the −log10 transformation of the FDR-adjusted p-value. Genes were classified according to FDR-adjusted p-value and $\log_2$ fold-change thresholds, and selected genes of biological interest were highlighted.

Functional enrichment analysis was performed using Gene Ontology (GO)-based Gene Set Enrichment Analysis (GSEA). DESeq2-derived differential expression results were used as input, and genes were ranked according to their $\log_2$ fold change values without applying a significance cutoff. Gene identifiers were converted from ENSEMBL IDs to Entrez Gene IDs and gene symbols using the org.Hs.eg.db annotation database, and duplicate identifiers were collapsed by retaining the gene with the highest absolute log2 fold change value.

GO-GSEA was performed using the gseGO() function implemented in the clusterProfiler R package [14]. Enrichment analysis was conducted for Biological Process (BP), Molecular Function (MF), and Cellular Component (CC) categories. Statistical significance was assessed using Benjamini–Hochberg multiple testing.

Table 1 Sequence of primers used in qRT-PCR analysis

Gene Name	Forward primer (5′→3′ sequence)	Reverse primer (5′→3′ sequence)
GAPDH	GTCAACGGATTTGGTCG TATTG	TGGAAGATGGTG ATGGGATTT
FER1L4	ACACAGTCCTTGTGGGT TCC	CCTGTCTCCTCCA TCTCTCC
MAMDC2	TACCAGCTTCAGCAGGGG	CCTCGTACAGGC CAGCCAT
ERBB4	GTTCAGGATGTGGACGT TGC	CTGCCGTCACAT TGTTCTGC
ADGRG1	GCGGGGAGGCTGAGAAG AGACT	CAGGCCAGGGCA GAGACGACACAG
GPM6A	ATCTCTGCTTGGACCTT CGT	CAGGCGTCTTTC ACATAGGC
DCDC2	AGAGAGGTCTGAAACA CGGG	CCTCCCTACCTCC TTCCTCT

RT-qPCR validation

Total RNA was extracted from independent biological replicates of untreated and 1 mM IAA-treated SH-SY5Y cells ($n=3$) using TRIzol Reagent [Invitrogen, Carlsbad, CA, US]. Genomic DNA removal and cDNA synthesis was carried out using the QuantiTect Reverse Transcription Kit [QIAGEN, Hilden, Germany]. qRT-PCR was carried out with the iQ SYBR green Supermix (Bio-Rad, Hercules, CA, USA) and the CFX96 System (Bio-Rad, Hercules, CA, USA). The thermocycling conditions were as follows: 2 min at 95 °C, 40 cycles of denaturation at 95 °C for 15 s and annealing at specific temperatures for 30 s, and extension for 20 s at 72 °C. Specific primer pairs used for this analysis were designed using Primer3 software (version 4.1.0, https://primer3.ut.ee) and are reported in Table 1. Relative expression was normalized to gene coding the glyceraldehyde-3-phosphate dehydrogenase (GAPDH) and calculated using the $2^{-\Delta\Delta Ct}$ method. Statistical significance was assessed by applying a two-tailed Student's t-test directly on ΔCt values. A p-value < 0.05 was considered statistically significant. Data wrangling, error propagation calculations, and statistical analyses were performed using R software (version 4.6.0) with the dplyr package.

Results and discussion

Principal component analysis (PCA) was performed on variance-stabilized normalized RNA-seq counts to evaluate global transcriptional differences among experimental conditions. The first two principal components accounted for 83% of the total variance, with PC1 and PC2 explaining 74% and 9% of the variability, respectively (Fig. 1). Biological replicates clustered closely within each condition, confirming the reproducibility of the RNA-seq dataset. Samples treated with 0.1 mM IAA showed a transcriptional profile closer to untreated controls, whereas samples exposed to 1 mM IAA displayed a marked separation along PC1 from both control and 0.1 mM IAA groups, indicating that the higher IAA concentration induced stronger global transcriptomic changes in SH-SY5Y cells. Consistent with the PCA results, differential expression analysis revealed a limited transcriptional effect at 0.1 mM IAA, with only one differentially expressed gene identified. Conversely, treatment with 1 mM IAA resulted in a stronger transcriptional response, with 113 differentially expressed genes identified based on an adjusted p-value ≤ 0.1 and an absolute log2 fold change > 1 (Fig. 2).

This concentration-dependent transcriptional response is consistent with the dose-dependent phenotypic effects previously reported for IAA in SH-SY5Y cells [4], where the

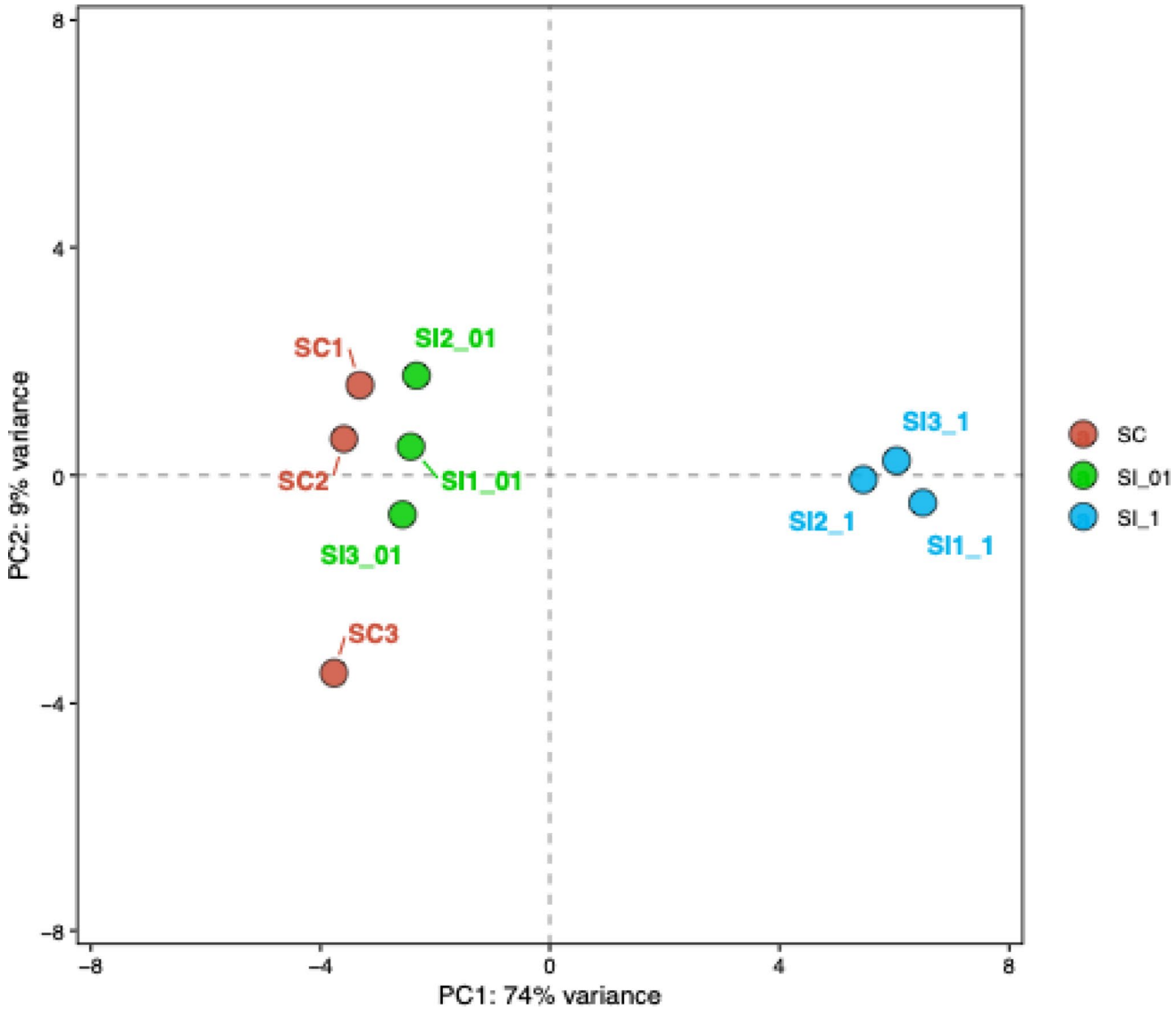


Fig. 1 Principal component analysis (PCA) of RNA-seq samples. PCA showing the distribution of three biological replicates for each experimental condition based on global transcriptomic profiles. S_Control, untreated SH-SY5Y cells; SI_01, SH-SY5Y cells treated with 0.1 mM indole-3-acetic acid (IAA); SI_1, SH-SY5Y cells treated with 1 mM IAA

antiproliferative and pro-autophagic effects were also more pronounced at 1 mM than at lower concentrations. Selected differentially expressed genes of biological relevance are reported in Table 2, including their log2 fold change values and adjusted p-values. In our previous investigation, we reported a clear time- and dose-dependent decrease in total ALK protein expression upon IAA treatment in SH-SY5Y cells. Interestingly, our transcriptomic dataset did not reveal statistically significant repression of ALK transcription at 48 h. This discrepancy between unchanged *ALK* transcript levels and previously reported reduced ALK protein levels is consistent with a post-transcriptional mode of regulation. One plausible hypothesis is that IAA promotes enhanced ALK protein degradation, potentially linked to the autophagic activity previously observed following IAA treatment; however, the present RNA-seq dataset does not establish protein degradation, nor does it identify autophagy as the mechanism responsible, and this hypothesis remains to be experimentally tested, for example through protein stability assays combined with pharmacological inhibition of autophagic or proteasomal degradation pathways.

In our previous study [4], IAA reduced cell viability in a concentration- and time-dependent manner in both SH-SY5Y and SK-N-BE(2) cells (*MYCN*-amplified, *PT53*-mutated), with significant effects at 0.1 and 1 mM after 48 and 72 h, i.6, in the concentration range used here. The effect was less pronounced in SK-N-BE(2), in line with neuroblastoma heterogeneity. The antiproliferative phenotype

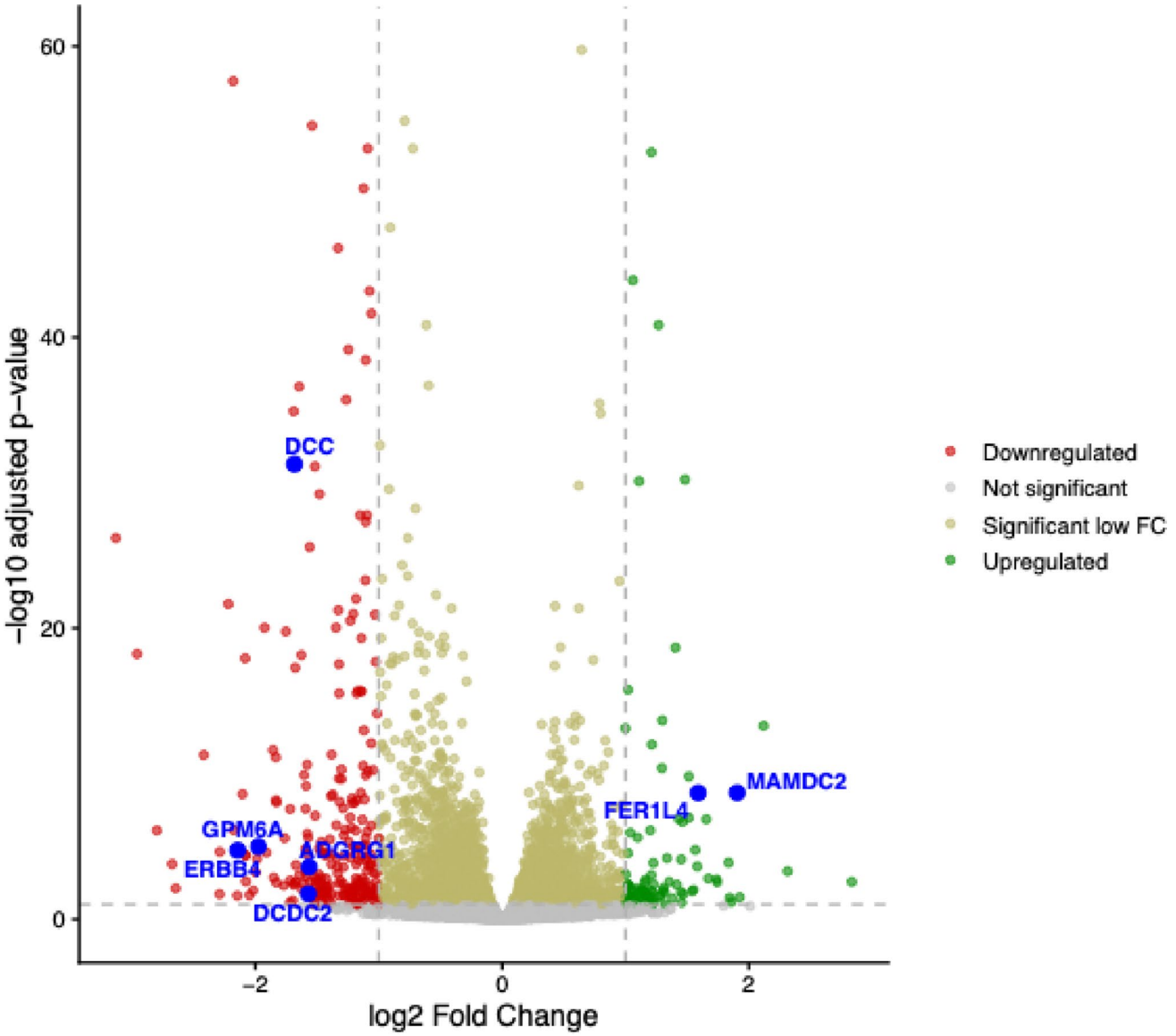


Fig. 2 Volcano plot showing differential gene expression changes in SH-SY5Y cells following IAA treatment compared with untreated controls. The x-axis represents the log2 fold change (IAA-treated vs. untreated), and the y-axis represents the −log10 transformation of the FDR-adjusted p-value. Genes with an adjusted p-value ≤ 0.1 and an absolute log2 fold change > 1 were classified as significantly upregulated (green) or downregulated (red). Genes meeting the adjusted p-value threshold but not the fold-change criterion are shown in khaki, whereas non-significant genes are shown in grey. Selected genes of biological relevance, based on their association with IAA-induced cellular responses and reported roles in cancer-related and neuronal processes, are highlighted and labelled

is therefore not restricted to a single neuroblastoma line; however, whether the transcriptional response described here is shared by SK-N-BE(2) or other models was not tested, and all transcriptomic findings are specific to SH-SY5Y. IAA has also been reported to reduce proliferation in Caco-2 intestinal epithelial cells [15–16], indicating that its antiproliferative effect is not restricted to SH-SY5Y cells.

GO-GSEA identified neuronal migration as a significantly enriched biological process, consistent with the neural crest origin of neuroblastoma and persistence of developmental migratory programs. This suggests that IAA treatment influences transcriptional programs related to the SH-SY5Y cell movement, cytoskeletal regulation, and neuronal developmental features, in line with its previous described effects on proliferation, migration, and clonogenicity [4].

ERBB4, *ADGRG1* (*GPR56*), *FER1L4*, and *MAMDC2* were selected as candidate genes based on their reported involvement in tumor-associated signalling, cellular behaviour, and processes relevant to the phenotype observed after IAA treatment.

To validate the RNA-seq findings, the relative expression levels of *FER1L4*, *MAMDC2*, *ERBB4*, *ADGRG1*, *GPM6A*,

Table 2 Differentially expressed genes tested by RNA-seq and qRT-PCR

Gene	$\log_2$ FC[a]	Adjusted *p*-value[b]	Relative level[c]	*p*-value[d]
FER1L4	1.58	2.11×10^{-9}	0.90	0.53
MAMDC2	1.90	2.07×10^{-9}	2.90	0.03
ERBB4	-2.14	1.91×10^{-5}	0.46	0.018
ADGRG1	-1.56	2.52×10^{-4}	1.2	0.71
DCC	-1.68	5.41×10^{-32}	n.d.	n.d.
GPM6A	-1.97	1.05×10^{-5}	0.48	0.046
DCDC2	-1.57	1.81×10^{-2}	1.0	0.79

[a]$\log_2$ FC, fold change based on $\log_2$; [b]Benjamini-Hochberg adjusted p-values for selected genes; [c]relative gene expression levels of selected genes from comparative CT method; $2^{-CT} > 1$, genes more highly expressed in SH-SY5Y cells treated for 48 h with 1 mM IAA; $2^{-CT} < 1$, genes more highly expressed in untreated SH-SY5Y cells; Two-tailed Student's t-test on ΔCt values; p-value < 0.05 was considered statistically significant. n.d., not determined. Values are the means ± SD of three different biological replicates. Data wrangling, error propagation calculations, and statistical analyses were performed using R software (version 4.6.0) with the dplyr package

and *DCDC2* were assessed by qRT-PCR in SH-SY5Y cells treated with 1 mM IAA (Table 2). Consistent with the RNA-seq data, *MAMDC2* was confirmed to be upregulated, while *ERBB4*, and *GPM6A* were confirmed to be downregulated following IAA treatment.

For *FER1L4*, *ADGRG1*, and *DCDC2* the variation did not reach statistical significance (Table 2); these genes are therefore reported as RNA-seq observations only, without independent validation. Overall, qRT-PCR confirmed the direction of change for three of the six genes tested (*ERBB4*, *GPM6A*, *and MAMDC2*) at the transcript level. Protein-level validation was not performed, as it falls outside the scope of this exploratory transcriptomic study and will be needed to confirm these findings.

ERBB4, a receptor tyrosine kinase involved in neuronal development and proliferative and survival signalling, was downregulated following IAA treatment. Reduced *ERBB4* expression or activity has been associated with attenuates *PI3K*/*AKT*-dependent signalling and reduced proliferation and survival in several cancer models [17–18], as well as high-risk neuroblastoma features [19]. Its downregulation of *ERBB4* is therefore consistent with our previous findings of reduced proliferation, G1 arrest, and clonogenic potential after IAA treatment, although this remains a correlative observation.

MAMDC2 downregulation in aggressive cancers correlates with *RAF*/*MEK*/*ERK* hyperactivation, whereas its re-expression promotes cell-cycle arrest; in breast cancer, *MAMDC2* has been reported to inhibit proliferation through this pathway [8]. Although these findings cannot be directly extrapolated to neuroblastoma, the robust induction of *MAMDC2* ($\log_2$ FC = 1.9), confirmed by RT-qPCR, is consistent with the G1 arrest and reduced clonogenicity observed in our functional assays [4], raising the hypothesis that it may restrain *RAF-ERK*/*AKT-ERK* signalling in SH-SY5Y cells. This remains speculative and require direct experimental testing.

The changes in *ADGRG1* (*GPR56*), *FER1L4* and *DCDC2* detected by RNA-seq (Table 2) were not confirmed by RT-qPCR; they are reported as RNA-seq observations only and are not considered further in the interpretation of the results.

Beyond their established roles in cancer-associated signalling, several of the modulated genes identified in our dataset are also involved in neuronal developmental processes, consistent with the neural origin of SH-SY5Y cells. In addition to *ERBB4*, other genes associated with neuronal migration were downregulated in the RNA-seq dataset: *GPM6A*, which was confirmed by RT-qPCR, and *DCC* and *DCDC2*, which are reported as RNA-seq observations only. *DCC* encodes a Netrin-1 receptor playing a central role in axonal guidance, neuronal migration, and cytoskeletal remodelling through intracellular signalling pathways regulating cell motility [20]. *GPM6A* contributes to neuronal differentiation, neurite extension, and neuronal membrane organization [21], whereas *DCDC2* is involved in microtubule organization and neuronal migration [22]. The downregulation of these genes is consistent with the GO-based GSEA results and suggests that IAA exposure is associated with transcriptional programs associated with neuronal migration, cytoskeletal dynamics, and neuronal cell-state regulation in SH-SY5Y cells. Given that SH-SY5Y cells retain neuronal lineage characteristics, the modulation of these developmental pathways may reflect a partial alteration of neural-related transcriptional programs rather than a direct effect on neuronal differentiation.

As an exploratory study, this work has a defined scope. The transcriptomic analysis was carried out in SH-SY5Y cells, and its extension to other neuroblastoma models, such as SK-N-BE(2) [4], will be of interest. RT-qPCR confirmed *MAMDC2*, *ERBB4* and *GPM6A*, whereas *ADGRG1*, *FER1L4* and *DCDC2* are reported as RNA-seq observations. Protein-level and functional analyses were beyond the scope of this work; the findings therefore describe transcript-level associations, and the candidate genes provide a basis for future mechanistic studies, including the hypothesized autophagy-related regulation of ALK. The millimolar IAA concentrations used are consistent with previous studies [4, 15, 16], and lower concentrations may be explored in future work.

Conclusions

Overall, the integration of RNA-seq and GO-based GSEA data indicates that IAA induces a coordinated transcriptional change in SH-SY5Y cells affecting genes involved

in proliferation, survival, adhesion, migration, and neuronal development-related processes. The concomitant modulation of *ERBB4*, *MAMDC2*, and *GPM6A*, confirmed by qRT-PCR, identified candidate molecular correlates compatible with the reduced proliferative, migratory, and clonogenic phenotype previously observed in IAA-treated SH-SY5Y cells, whereas *ADGRG1*, *FER1L4* and *DCDC2* are reported as RNA-seq observations only. These findings support a role for IAA as a modulator of SH-SY5Y neuroblastoma cell transcriptional states and identify a set of candidate genes and pathways warranting further mechanistic investigation. As discussed above, the causal contribution of these genes, the generalizability of these findings beyond the SH-SY5Y model, protein-level validation, and the proposed autophagy-related mechanism of *ALK* regulation remain to be experimentally established.

Acknowledgements The authors gratefully acknowledge Marco Petruzziello, Franca Senecione, and Valentina Brasiello for technical support.

Author contributions C.B., A.V., A.D., and E.N. conceptualized the study; S.V., M.L.A., R.M., R.Mat., and M.M. carried out the sperimental activities; S.V., M.L.A., R.M., R.Mat. performed the data Aalysis; C.B., A.V., S.V., A.D., and E.N. have written, revised and edited the manuscript; C.B., and A.V. supervised the study; C.B., and A.V. provided the funds.

Funding This study was supported by the Ministero dell'università e della ricerca, PRIN P2022585CF.

Data availability No datasets were generated or analysed during the current study.

Declarations

Competing interests The authors declare that they have no known competing financial interests or personal relationships that could have appeared to influence the work reported in this paper.

References

1. Tsubota S, Kadomatsu K (2018) Origin and initiation mechanisms of neuroblastoma. Cell Tissue Res 372:211–221
2. Wang Y, Zhao Z, Wang J et al (2026) Advances in multi-omics research on neuroblastoma. Front Pediatr 14:1739376. https://doi.org/10.3389/fped.2026.1739376
3. Perri P, Ponzoni M, Corrias MV et al (2021) A focus on regulatory networks linking MicroRNAs, transcription factors and target genes in neuroblastoma. Cancers 13:5528
4. Mallardo M, Nigro E, Bianco C et al (2025) Insights from an in vitro study: the anti-proliferative effects of indole-3-acetic acid in neuroblastoma cells. Biochem Pharmacol 117231 https://doi.org/10.1016/j.bcp.2025.117231
5. El-Gamal MI, Mewafi NH, Abdelmotteleb NE et al (2021) A Review of HER4 (ErbB4) Kinase, Its Impact on Cancer, and Its Inhibitors. Molecules 26:7376. https://doi.org/10.3390/molecules26237376
6. Aust G, Zhu D, Van Meir EG, Xu L (2016) Adhesion GPCRs in Tumorigenesis. In: Langenhan T, Schöneberg T (eds) Adhesion G Protein-coupled Receptors. Springer International Publishing, Cham, pp 369–396
7. Xia T, Chen S, Jiang Z et al (2015) Long noncoding RNA FER1L4 suppresses cancer cell growth by acting as a competing endogenous RNA and regulating PTEN expression. Sci Rep 5:13445
8. Lee H, Park B-C, Soon Kang J et al (2020) MAM domain containing 2 is a potential breast cancer biomarker that exhibits tumour-suppressive activity. Cell Prolif 53:e12883
9. Defez R, Valenti A, Andreozzi A et al (2019) New Insights into Structural and Functional Roles of Indole-3-acetic acid (IAA): Changes in DNA Topology and Gene Expression in Bacteria. Biomolecules 9:522. https://doi.org/10.3390/biom9100522
10. Deng Z-L, Münch PC, Mreches R, McHardy AC (2022) Rapid and accurate identification of ribosomal RNA sequences via deep learning. Nucleic Acids Res 50:e60–e60
11. Chen S, Zhou Y, 11., Chen Y, Gu J (2018) fastp: an ultra-fast all-in-one FASTQ preprocessor. Bioinformatics 34:i884–i890
12. Dobin A, Davis CA, Schlesinger F et al (2013) STAR: ultrafast universal RNA-seq aligner. Bioinformatics 29:15–21
13. Love MI, Huber W, Anders S (2014) Moderated estimation of fold change and dispersion for RNA-seq data with DESeq2. Genome Biol 15:550
14. Yu G, Wang L-G, Han Y, He Q-Y (2012) clusterProfiler: an R package for comparing biological themes among gene clusters. OMICS 16:284–287
15. Mallardo M, Memon F, Pagliaro R et al (2026) Indole-3-acetic acid promotes differentiation while suppressing proliferation in human intestinal epithelial cells. Hum Cell 39:87. https://doi.org/10.1007/s13577-026-01397-x
16. Tomii A, Higa M, Naito K et al (2023) Activation of the TLR4-JNK but not the TLR4-ERK pathway induced by indole-3-acetic acid exerts anti-proliferative effects on Caco-2 cells. Biosci Biotechnol Biochem 87:839–849. https://doi.org/10.1093/bbb/zbad055
17. Xu J, Gong L, Qian Z et al (2018) ERBB4 promotes the proliferation of gastric cancer cells via the PI3K/Akt signaling pathway. Oncol Rep 39:2892–2898
18. Anfield K, Li J, Wilkins OM et al (2015) Receptor tyrosine kinase ERBB4 mediates acquired resistance to ERBB2 inhibitors in breast cancer cells. Cell Cycle 14:648–655
19. Miao L, Wang H-Y, Zheng M-N et al (2026) Single-cell transcriptomic atlas-guided NRG3-ERBB4 axis enhances the efficacy of chemo-immunotherapy during induction phase in high-risk neuroblastoma. Mol Ther 34:4243–4260. https://doi.org/10.1016/j.ymthe.2026.04.031
20. Yamagishi S, Bando Y, Sato K (2021) Involvement of netrins and their receptors in neuronal migration in the cerebral cortex. Front cell Dev biology 8:590009
21. Huang B, Li X (2025) Mechanisms of GPM6A in malignant tumors. Cancer Rep 8:e70137
22. Wan W, Li Y, Sun W et al (2025) The DCDC2/ENO1 axis promotes tumor progression and immune evasion in intrahepatic cholangiocarcinoma via activating FGL1-LAG3 checkpoint. J Exp Clin Cancer Res 44:177. https://doi.org/10.1186/s13046-025-03436-1

Publisher's note Springer Nature remains neutral with regard to jurisdictional claims in published maps and institutional affiliations.

Springer Nature or its licensor (e.g. a society or other partner) holds exclusive rights to this article under a publishing agreement with the author(s) or other rightsholder(s); author self-archiving of the accepted manuscript version of this article is solely governed by the terms of such publishing agreement and applicable law.